Published April 8, 2024 as 10.3174/ajnr.A8276

ORIGINAL RESEARCH

Head and Neck imaging

Comparison of Image Quality and Radiation Dose in Pediatric Temporal Bone CT using Photon Counting Detectors CT and Energy Integrating Detectors CT

Jeong Sub Lee, John Kim, Jayapalli R. Bapuraj, and Ashok Srinivasan

ABSTRACT

BACKGROUND AND PURPOSE: To compare the image quality and radiation dose of temporal bone CT scans in pediatric patients acquired with photon counting detectors (PCD) CT and energy integrating detectors (EID) CT.

MATERIALS AND METHODS: The retrospective study included a total of 110 pediatric temporal bone CT scans (PCD-CT, n=52; EID-CT, n=58). Two independent readers evaluated the spatial resolution of 4 anatomical structures (tympanic membrane, incudostapedial joint, stapedial crura, and cochlear modiolus) and overall image quality using a 4-point scale. Inter-reader agreement was assessed. Dose length product (DLP) for each CT was compared, and subgroup analyses were performed based on age (under 3 years, 3-5 years, 6-11 years, and 12 years and above).

RESULTS: PCD-CT demonstrated statistically significantly higher scores than EID-CT for all items (tympanic membrane, 2.9 vs. 2.4; incudostapedial joint, 3.6 vs. 2.6, stapedial crura, 3.2 vs. 2.4; cochlear modiolus, 3.4 vs. 2.8; overall image quality, 3.6 vs. 2.8; p<0.05). Inter-reader agreement ranged from good to excellent (ICCs, 0.6-0.81). PCD-CT exhibited a 43% dose reduction compared to EID-CT, with a particularly substantial reduction of over 70% in the subgroups of children under 6 years.

CONCLUSIONS: PCD temporal bone CT achieves significantly superior imaging quality at a lower radiation dose compared to EID-CT.

ABBREVIATIONS: PCD-CT = photon counting detectors CT; EID-CT = energy integrating detectors CT; DLP = dose length product; AEC = automatic exposure control; ICC = interclass correlation coefficient.

Received month day, year; accepted after revision month day, year.
From the Department of Radiology (J.L.), Jeju National University Hospital, Jeju National University college of medicine, Jeju-si, Jeju-do, Republic of Korea; Department of Radiology (J.K., J.R.B., A.S.), University of Michigan, Ann Arbor, Michigan, U.S.A.

The authors declare no conflicts of interest related to the content of this article.

Please address correspondence to John Kim, M.D., Department of Radiology, University of Michigan, 1500 E. Medical Center Dr., B2A205A, Ann Arbor, MI, 48109-5030, U.S.A.; e-mail: johannk@med.umich.edu.

SUMMARY SECTION

PREVIOUS LITERATURE: According to previous studies using adult or cadaveric models, PCD-CT can obtain images of better quality compared to EID-CT due to the characteristics of the detector, and it can also reduce radiation dose. However, there is currently a lack of research directly comparing PCD-CT and EID-CT in pediatric temporal bone CT imaging.

KEY FINDINGS: PCD-CT exhibited significantly better subjective spatial resolution and overall image quality compared to EID-CT (p<0.05). The radiation dose was reduced by 43.3% with PCD-CT compared to EID-CT, with particularly over 70% reduction observed in subgroups aged under 6.

KNOWLEDGE ADVANCEMENT: In pediatric temporal bone CT, PCD-CT can obtain better images with less radiation dose. This will be of great benefit in the diagnostic imaging of pediatric patients.

INTRODUCTION

A high spatial resolution image is necessary for distinguishing small internal structures in temporal bone CT [1, 2]. However, the need to obtain high resolution images should be balanced with the need to limit radiation dose, especially in pediatric patients.

Conventional energy integrating detectors CT (EID-CT) utilizes a scintillator layer to convert X-rays into visible light, and then a photodiode converts it back into an electric signal. This process requires septa, which hinders maximal achievable spatial resolution [3-5].

Photon counting detector CT (PCD-CT) is the most recently commercialized CT technology. In contrast to EID-CT, PCD-CT differs in that it utilizes semiconductor detector materials without a scintillator layer to convert X-rays into electronic signals [6-8]. A PCD can measure the number and energy of X-ray photons and is not dependent on energy-weighting. Thus, lower energy X-ray thresholds can be selected to improve iodine or soft tissue contrast [5, 7, 9, 10]. Additionally, material decomposition can be achieved with a single X-ray tube and various

Copyright 2024 by American Society of Neuroradiology.

reconstructions such as virtual noncontrast and virtual monochromatic images can also be created. Unlike EID-CT, it lacks detector septa, enabling image acquisition with a smaller pixel size and better spatial resolution. The removal of electronic noise also allows for the application of ultra-low dose CT protocols, presenting an advantage [5, 11].

Prior temporal bone imaging studies in cadaveric models and adult patients have shown reduced radiation dose and superior spatial resolution with PCD-CT compared to EID-CT. However, there is currently no comparative study specifically focused on pediatric patients [3, 12-15].

Therefore, the aim of this study is to compare the image quality and radiation dose of pediatric temporal bone CT obtained with PCD-CT and EID-CT.

MATERIALS AND METHODS

Patients

This retrospective study received approval from our institutional review board (IRB No. 00244315), and informed consent was waived. The study included 61 consecutive pediatric patients under the age of 18 who underwent temporal bone CT scans from April 2023 to November 2023 using PCD-CT (Naeotom Alpha, Siemens Healthineers, Forchheim, Germany), as well as 64 consecutive pediatric patients who underwent temporal bone imaging from September 2022 to March 2023 using conventional EID-CT (Discovery HD750, General Electric, Waukesha, WI, USA).

CT protocol

Table 1 shows the scan parameters for both CT scanners. For PCD-CT, to adjust radiation dose, protocols were varied based on a 6-year-old reference and all scans were conducted in high-resolution mode. Automatic exposure control (AEC) software, including CARE Dose 4D and CARE kV were used. For EID-CT, scan parameters were adjusted for three groups: those under 3 years old, those between 3 and 11 years old, and those aged 12 and above, with all scans performed in high-resolution mode. Fixed mA was employed instead of using AEC software.

Image review

All images were reconstructed into axial, coronal, and sagittal planes. Two board-certified radiologists with 5 (J.L.) and 14 (J.K.) years of temporal bone imaging experience independently and blindly reviewed the images of PCD-CT and EID-CT using PACS (Sectra Workstation IDS7, Linköping, Sweden). Subjective spatial resolution and image quality was assessed for 4 anatomical structures (tympanic membrane, incudostapedial joint, stapedial crura, and cochlear modiolus) using a 4-point Likert scale: 1 = inferior resolution with degraded visualization, 2 = slightly inferior resolution without affecting visualization, 3 = slightly superior resolution without affecting visualization, 4 = superior resolution with improved visualization (Figure 1). The assessment of structures was conducted by selecting the best visualized or most normal side of the temporal bone CT. After all the patients had been evaluated and scored, for structures that were deemed unassessable (e.g., fluid in the middle cavity obscuring the tympanic membrane), consensus was reached by both observers for their exclusion. Unassessable structures were excluded while unaffected remaining structures were included. Additionally, overall image quality was evaluated using a 4-point Likert scale: 1= poor image quality with degraded diagnostic performance, 2= fair image quality without degraded diagnostic performance, 3= good image quality without significant image quality disturbance, 4= excellent image quality without image quality disturbance.

Radiation Dose

Radiologist J.L. extracted the radiation dose details from the dose reports of individual patients that had already been included on PACS as part of their imaging records, and compared the dose length product (DLP) between the two groups. Since protocol adjustments for radiation dose reduction were based on different age ranges for the two CT scanners, we divided the study population into 4 subgroups (under 3 years, 3-5 years, 6-11 years, and 12 years and above) and compared the average DLP within each subgroup.

Statistical Analysis

Age, weight, DLP, and Liker scales for quality analysis were compared using mean values for each CT group, with the statistical significance of these variables determined through t-test. In subgroup analyses, as the values did not adhere to a normal distribution, the Mann-Whitney U test was used. Sex distribution between the two patient groups was assessed using a chi-square test. To assess the inter-reader agreement, the intraclass correlation coefficient (ICC) was used. The agreement was categorized as poor (<0.40), fair (0.40-0.59), good (0.60-0.75), and excellent (>0.75). A p-value less than 0.05 was considered statistically significant. The statistical analysis was conducted using SPSS version 20 (IBM corporation, Armonk, NY, USA).

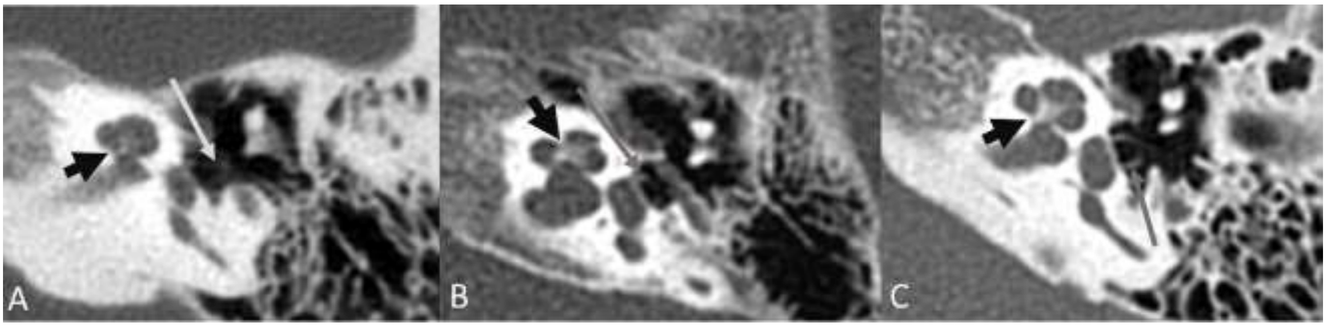

FIG 1. Likert scale examples of subjective spatial resolution for different patients (A, EID-CT; B-C, PCD-CT). The stapedial crus

(long arrow) and cochlear modiolus (short arrow) are rated as 2 points in A, 3 points in B, and 4 points in C, respectively.

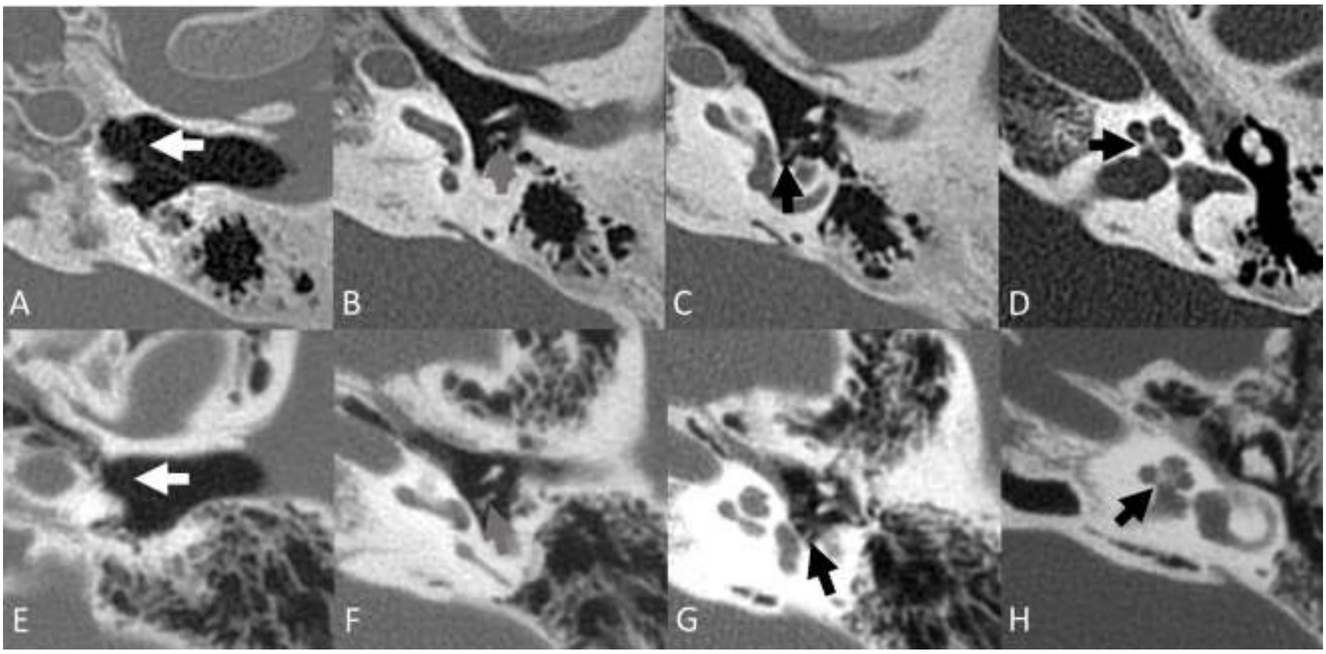

FIG 2. (A-D) Left temporal bone CT images of a 14-year-old male from PCD-CT. The axial CT images show anatomical structures, including the tympanic membrane (A, arrow), incudostapedial joint (B, arrow), stapedial crus (C, arrow), and cochlear modiolus (D, arrow). Both readers rated a score of 4 for all anatomical structures and overall image quality.

(E-H) Left temporal bone CT images of a 13-year-old female from EID-CT. The axial CT images show anatomical structures, including the tympanic membrane (E, arrow), incudostapedial joint (F, arrow), stapedial crus (G, arrow), and cochlear modiolus (H, arrow). Both readers rated a score of 3 for incudostapedial joint, cochlear modiolus, and overall image quality. And tympanic membrane and stapedial crura were rated a score of 2 and 4, respectively.

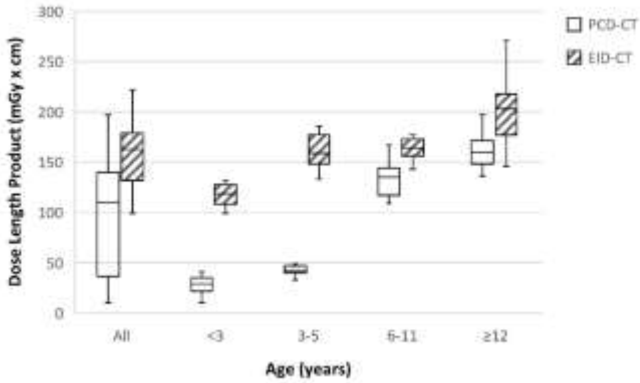

FIG 3. Box-plot graphs for the dose-length products of photon counting detectors CT and energy integrating detectors CT in age-related subgroups.

RESULTS

Among the 125 enrolled patients, twelve patients (PCD-CT, n=6; EID-CT, n=6) who were imaged using only a contrast-enhanced protocol without precontrast images, and three patients (PCD-CT) who did not have high resolution temporal bone images were excluded from the study. A total of 110 patients were included (PCD-CT, n=52; EID-CT, n=58), with reasons for examination being hearing loss (n=65), inflammation or infection (n=26), congenital malformation (n=9), and miscellaneous reasons (i.e., mass, trauma, hyperacusis, dizziness, etc.; n=10). Patient characteristics are presented in table 2. There were no statistically significant differences in the mean age, gender distribution, and weight between PCD-CT and EID-CT groups ($p>0.05$). Within the subgroups divided by age, there were no statistically significant differences in mean weight of the populations between the two CT groups ($p>0.05$).

Table 3 shows subjective spatial resolution and image quality scores for the 4 anatomical structures and overall image quality. PCD-CT exhibited significantly higher scores than EID-CT for all assessed items ($p<0.05$, Figures 2). PCD-CT exhibited values exceeding a mean of 3.0 for all items except the tympanic membrane, whereas EID-CT scored below a mean of 3.0 for all items. In the tympanic membrane, both CT scans exhibited the lowest scores, with the mean difference being relatively the smallest (2.9±1.1 vs. 2.4±0.7, $p=0.022$). The highest-scoring items were the incudostapedial joint and overall image quality for PCD-CT, and the average score difference between these items for the two CT scans was relatively large (3.6±0.7 vs. 2.6±0.5, 3.6±0.6 vs. 2.8±0.3, $p<0.001$, respectively). The inter-reader agreement for spatial resolution scores for each item indicated good or excellent agreement in both CT scans (ICCs, 0.6-0.81, table 4).

Table 5 shows DLP for both CT scans. The mean DLP (mGy x cm) showed significantly lower values on PCD-CT compared to EID-CT (91.3±57.1 vs. 161.0±35.9, $p<0.001$). When comparing age-related subgroups, PCD-CT consistently demonstrated lower mean values across all age subgroups ($p<0.01$, Figure 3). In the overall group, PCD-CT exhibited a dose reduction of approximately 43% compared to EID-CT. Particularly, PCD-CT exhibited a significantly substantial dose reduction (72-77%) compared to EID-CT in the age groups of less than 6 years.

DISCUSSION

In this study, PCD-CT demonstrated superior subjective spatial resolution and image quality in pediatric temporal bone imaging compared to EID-CT, with an additional advantage of lower radiation dose. This study demonstrated consistent results with previous studies, supporting the notion that PCD-CT provides better image quality and high-resolution images compared to conventional EID-CT. The ability of PCD-CT to achieve thinner slice thickness is considered to be one of the primary factors contributing to this [12].

The tympanic membrane, being a thin structure challenging to visualize distinctly in CT, scored the lowest in both CT scans. However, in PCD-CT, it presented a relatively improved subjective spatial resolution with an average score close to 3.0 (slightly superior resolution without affecting visualization). While EID-CT yielded scores below a mean of 3.0 for all items (2.4-2.8), PCD-CT showed values exceeding a mean of 3.5 for most items, indicating improved resolution. In previously published studies, spatial resolution scores evaluated for anatomical structures were significantly higher in PCD-CT, and image quality scores were also superior [3, 13, 15].

Regarding radiation dose, PCD-CT demonstrates a significant reduction compared to EID-CT in pediatric temporal bone imaging. Benson et al. reported a 31% dose reduction in a study involving 13 adult patients [3], and Hermans et al. showed a 26% dose reduction in a study with 36 adults [13]. In this study, a protocol identical to that used for adults was applied to subgroups aged 6 and above, PCD-CT exhibited a dose reduction of around 20%, similar to previous studies. Particularly, in the subgroups under 6 years, where the dose was set even lower in PCD-CT, a dose reduction of over 70% compared to EID-CT was achievable. The radiation sensitivity is greater in children than in adults, increasing with younger age [16]. Therefore, the significance of this study lies in demonstrating the advantage of PCD-CT, which can obtain superior image quality and spatial resolution with significantly lower radiation doses, especially in young pediatric patients.

This study has the following limitations. Firstly, it employed a retrospective study design with a small sample size. However, to our knowledge, this is the first dedicated pediatric and largest cohort of temporal bone CT evaluations to date described in the literature. Secondly, although the radiologists were blinded to the type of images, the superior and sharper appearing PCD-CT may be a giveaway and cannot be concealed by any imaging subterfuge. Thirdly, this study focused on only normal structures. However, the notable resolution improvement of PCD-CT suggests its potential utility in observing small structures in pediatric patients for the assessment of pathology or anatomical anomalies. Furthermore, the image evaluations were compared using subjective assessment techniques, and it should be noted that different age-based dose reduction protocols were applied for the two CT scans. In an ideal situation, a prospective randomized study comparing the two CT modalities would be the preferred design, including quantitative analysis, and the authors hope that this endeavor would be the first step in recognizing the superiority of PCD-CT.

Table 1: Scan parameters for photon counting detectors CT (PCD-CT) and energy integrating detectors CT (EID-CT).

	PCD-CT		EID-CT		
	<6 yr	≥6 yr	<3 yr	3-11 yr	≥12 yr
Tube voltage (kVp)	90(ref)	120 (ref)	120	120	120
Tube current	58mAs (quality ref)	99mAs (quality ref)	100mA	120mA	150mA
Image quality matrix	IQ 42	IQ 110	-	-	-
Matrix size	768x768	768x768	512x512	512x512	512x512
Pitch	0.85	0.85	0.531	0.531	0.531
Gantry rotation time	0.5	0.5	0.5	0.5	0.5
Collimation	120x0.2mm	120x0.2mm	64x0.675mm	64x0.675mm	64x0.675mm
Kernel	Hr72	Hr72	HD bone	HD bone	HD bone
Iterative reconstruction	QIR off	QIR off	AR30	AR30	AR30
Slince thickness	0.3mm	0.3mm	0.625mm	0.625mm	0.625mm
Interval	0.3mm	0.3mm	0.312mm	0.312mm	0.312mm
Automatic exposure control	Used	Used	None	None	None

Ref= reference

Table 2: Patient characteristics on photon counting detectors CT (PCD-CT) and energy integrating detectors CT (EID-CT)

	PCD-CT (n=52)	EID-CT (n=58)	P value
Age (yr)	6.2±4.3	6.9±5.5	0.466
Sex (male/ female)	24/28	31/27	0.445
Weight (kg)	29.0±22.1	30.6±24.0	0.705

Data, excluding sex, are presented as mean ± standard deviation. Statistical significance is set at $p<0.05$.

Table 3: Subjective spatial resolution and image quality scores of photon counting detectors CT (PCD-CT) and energy integrating detectors CT (EID-CT).

	Tympanic membrane	Incudostapedial joint	Stapedial crura	Cochlear modiolus	Overall image quality
Reader 1 PCD-CT	2.9±0.9	3.7±0.6	3.1±0.8	3.7±0.8	3.6±0.7
EID-CT	2.4±0.7	2.5±0.6	2.2±0.6	2.8±0.5	2.8±0.4
p-value	0.001	<0.001	<0.001	<0.001	<0.001

Reader 2	PCD-CT	3.4±0.6	3.7±0.6	3.4±0.7	3.8±0.4	3.7±0.6
	EID-CT	2.7±0.6	2.8±0.5	2.6±0.7	3.0±0.4	2.9±0.3
	p-value	<0.001	<0.001	<0.001	<0.001	<0.001
Mean	PCD-CT	2.9±1.1	3.6±0.7	3.2±0.8	3.4±1.1	3.6±0.6
	EID-CT	2.4±0.7	2.6±0.5	2.4±0.6	2.8±0.6	2.8±0.3
	p-value	0.022	<0.001	<0.001	<0.001	<0.001

Data are presented as mean ± standard deviation. Statistical significance is set at p<0.05.

Table 4: Inter-reader agreement with interclass correlation coefficient (ICC) for subjective spatial resolution scores.

	PCD-CT		EID-CT	
	ICC (2,1)	95% CI	ICC (2,1)	95% CI
Tympanic membrane	0.631	0.223-0.812	0.661	0.358-0.813
Incudostapedial joint	0.773	0.602-0.870	0.630	0.309-0.794
Stapedial crura	0.664	0.401-0.810	0.640	0.265-0.810
Cochlear modiolus	0.630	0.344-0.792	0.634	0.381-0.784
Overall image quality	0.808	0.667-0.890	0.632	0.379-0.782
Tympanic membrane	0.631	0.223-0.812	0.661	0.358-0.813

Table 5: Inter-reader agreement with interclass correlation coefficient (ICC) for subjective spatial resolution scores.

Age (years)	PCD-CT (n=52)	EID-CT (n=58)	P value	Reduction rate
All	91.3 ± 57.1	161.0 ± 35.9	<0.001	43.3%
< 3	27.8 ± 8.4 (n=13)	119.9 ± 15.9 (n=16)	<0.001	76.8%
3-5	44.2 ± 9.7 (n=10)	159.4 ± 16.9 (n=11)	<0.001	72.3%
6-11	129.3 ± 3.0 (n=23)	163.5 ± 10.3 (n=14)	<0.001	20.9%
≥ 12	161.2 ± 20.1 (n=6)	198.6 ± 29.6 (n=17)	0.006	18.8%

Data are presented as mean ± standard deviation. Statistical significance is set at p<0.05.

CONCLUSIONS

In conclusion, PCD-CT can significantly reduce radiation dose while providing superior spatial resolution and image quality in pediatric temporal bone CT, making it a valuable imaging asset for the management of pediatric patients.

REFERENCES

1. Lane JI, Lindell EP, Witte RJ, et al. Middle and inner ear: improved depiction with multiplanar reconstruction of volumetric CT data. Radiographics 2006;26:115-124
2. Leng S, Diehn FE, Lane JI, et al. Temporal Bone CT: Improved Image Quality and Potential for Decreased Radiation Dose Using an Ultra-High-Resolution Scan Mode with an Iterative Reconstruction Algorithm. AJNR Am J Neuroradiol 2015;36:1599-1603
3. Benson JC, Rajendran K, Lane JI, et al. A New Frontier in Temporal Bone Imaging: Photon-Counting Detector CT Demonstrates Superior Visualization of Critical Anatomic Structures at Reduced Radiation Dose. AJNR Am J Neuroradiol 2022;43:579-584
4. Flohr T, Petersilka M, Henning A, et al. Photon-counting CT review. Phys Med 2020;79:126-136
5. Esquivel A, Ferrero A, Mileto A, et al. Photon-Counting Detector CT: Key Points Radiologists Should Know. Korean J Radiol 2022;23:854-865
6. Rajendran K, Petersilka M, Henning A, et al. First Clinical Photon-counting Detector CT System: Technical Evaluation. Radiology 2022;303:130-138
7. Leng S, Bruesewitz M, Tao S, et al. Photon-counting Detector CT: System Design and Clinical Applications of an Emerging Technology. Radiographics 2019;39:729-743
8. Willemink MJ, Persson M, Pourmorteza A, et al. Photon-counting CT: Technical Principles and Clinical Prospects. Radiology 2018;289:293-312
9. Gutjahr R, Halaweish AF, Yu Z, et al. Human Imaging With Photon Counting-Based Computed Tomography at Clinical Dose Levels: Contrast-to-Noise Ratio and Cadaver Studies. Invest Radiol 2016;51:421-429
10. Pourmorteza A, Symons R, Reich DS, et al. Photon-Counting CT of the Brain: In Vivo Human Results and Image-Quality Assessment. AJNR Am J Neuroradiol 2017;38:2257-2263
11. Leng S, Rajendran K, Gong H, et al. 150-mum Spatial Resolution Using Photon-Counting Detector Computed Tomography Technology: Technical Performance and First Patient Images. Invest Radiol 2018;53:655-662
12. Cao J, Bache S, Schwartz FR, et al. Pediatric Applications of Photon-Counting Detector CT. AJR Am J Roentgenol 2023;220:580-589
13. Hermans R, Boomgaert L, Cockmartin L, et al. Photon-counting CT allows better visualization of temporal bone structures in comparison with current generation multi-detector CT. Insights Imaging 2023;14:112
14. Rajendran K, Voss BA, Zhou W, et al. Dose Reduction for Sinus and Temporal Bone Imaging Using Photon-Counting Detector CT With an Additional Tin Filter. Invest Radiol 2020;55:91-100
15. Zhou W, Lane JI, Carlson ML, et al. Comparison of a Photon-Counting-Detector CT with an Energy-Integrating-Detector CT for Temporal Bone Imaging: A Cadaveric Study. AJNR Am J Neuroradiol 2018;39:1733-1738
16. Alzen G, Benz-Bohm G. Radiation protection in pediatric radiology. Dtsch Arztebl Int 2011;108:407-414
17. Siegel MJ, Bugenhagen SM, Sanchez A, et al. Comparison of Radiation Dose and Image Quality of Pediatric High-Resolution Chest CT Between Photon-Counting Detector CT and Energy-Integrated Detector CT: A Matched Study. AJR Am J Roentgenol 2023;221:363-371

SUPPLEMENTAL FILES